STORAGE RING AND INTERACTION REGION MAGNETS FOR A μ+μ- HIGGS FACTORY*

A.V. Zlobin#, Y.I. Alexahin, V.V. Kapin, V.V. Kashikhin, N.V. Mokhov, S.I. Striganov,
I.S. Tropin, FNAL, Batavia, IL 60510, USA

Abstract

A low-energy Muon Collider (MC) offers unique opportunities to study the recently found Higgs boson. However, due to a relatively large beam emittance with moderate cooling in this machine, large-aperture high-field superconducting (SC) magnets are required. The magnets need also an adequate margin to operate at a large radiation load from the muon decay showers. General specifications of the SC dipoles and quadrupoles for the 125 GeV c.o.m. Higgs Factory with an average luminosity of ~$2 \cdot 10^{31}$ cm^{-2}s^{-1} are formulated. Magnet conceptual designs and parameters are reported. The impact of the magnet fringe fields on the beam dynamics as well as the IR and lattice magnet protection from radiation are also reported and discussed.

INTRODUCTION

The major advantage of a μ+μ- collider-based Higgs Factory (HF) [1] is the possibility of direct precise measurement of the Higgs boson mass and width. According to the general concept of such a machine [2], muons - in order to keep their longitudinal emittance and energy spread low - undergo only partial cooling leaving their transverse emittance relatively high (see Table 1). Therefore quite small values (a few cm) of the β-function at the Interaction Point (IP) are required resulting in a large beam size in the Final Focus (FF) quadrupoles.

Together with the necessity of magnets and detector protection from the muon decay showers, this leads to very large magnet apertures imposing challenging engineering constraints for magnet design and creating beam dynamics issues with magnet field quality and fringe fields.

Table 1: Higgs Factory Parameters

Parameter	Unit	Value
Circumference	m	300
Beam energy	GeV	62.5
Transverse emittance, $\varepsilon_{\perp N}$	(π)mm·rad	0.3
Longitudinal emittance, $\varepsilon_{\parallel N}$	(π)mm·rad	1.0
Beam energy spread	%	0.003
β*	cm	2.5
Repetition rate	Hz	30
Muons/bunch	-	2×10^{12}
Average luminosity	cm^{-2}s^{-1}	2.5×10^{31}

Table 1 gives basic parameters of the HF Storage Ring (SR) preliminary design presented in [3]. The conceptual

design and analysis of the Interaction Region (IR) large-aperture magnets has shown that the IR magnets with apertures ~500 mm and operation fields ~12 T are feasible using the Nb$_3$Sn technology.

This paper continues the design studies of the HF IR and SR magnets. The impact of the magnet field quality and fringe fields on the beam dynamics, the IR and lattice magnet protection from radiation are also discussed.

STORAGE RING LATTICE

The HF lattice layout and the beam sizes are shown in Fig. 1 for parameters given in Table 1. The IR includes FF quadruplet (with first quadrupole Q1 at 3.5 m from IP) and dipoles generating dispersion for subsequent 3-sextupole chromaticity correction [4]. The latter is necessary despite small energy spread to compensate the path length increase due to betatron oscillations. The matching section allows for β* variation in wide range.
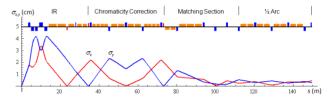

Figure 1: Layout and beam sizes in HF half-ring. Quadrupole magnets are shown in blue, dipoles in orange and sextupole correctors in red color.

MAGNET REQUIREMENTS

Table 2 shows the IR magnet parameters discussed in [3]. The orbit sagitta in IR dipoles is quite large – 8.1 cm. However, it does not affect the IR dipole bore diameter since it is determined by a large vertical beam size.

Table 2: IR Magnet Specifications

Parameter	Q1	Q2	Q3	Q4	B1
$10\sigma_{max}$ (mm)	234	411	339	415	405
G_{nom} (T/m)	74	-36	44	-25	0
B_{nom} (T)	0	2	0	2	8
L_{mag} (m)	1.00	1.40	2.05	1.70	4.10
Coil aperture (mm)	267	444	372	448	438
Quantity	1	2	1	1	2

Tables 3-4 present the maximum values of main parameters for the dipoles (B) and quadrupoles (Q) used in the chromaticity section (CS), the matching section (MS) and the arc (ARC). The most challenging magnets are the CS dipoles (B_{CS}), some MS dipoles (B_{MS}I) and the arc dipoles (B_{ARC}) which need high nominal operation field up to 10 T. This field level requires using the Nb$_3$Sn technology.

The magnet aperture outside the IR region reduces from 231 mm in CS quadrupoles to 92 mm in arc dipoles. Note, that the aperture size in the arc is defined by the arc dipoles due to a relatively large beam sagitta. To standardize the magnet designs in different sections it was decided to use for this study two different aperture sizes – large ~231 mm in CS and adjacent part of MS, and small ~130 mm in ARC and adjacent part of MS.

Table 3: SR Dipole Magnet Specifications

Parameter	B_{CS}	$B_{MS}I$	$B_{MS}II$	B_{ARC}
$10\sigma_{max}$ (mm)	225	222	127	92
B_{nom} (T)	10	10	6.4	10
L_{mag} (m)	1.8	2.4	3.6	3.0
Coil aperture (mm)	258	255	160	120
Quantity	13	2	3	8

Table 4: SR Quadrupole Magnet Specifications

Parameter	Q_{CS}	Q_{MS}	Q_{ARC}
$10\sigma_{max}$ (mm)	231	130	46
B_{nom} coil (T)	5.3	5.5	3.3
Length (m)	1.0	1.0	1.0
Coil aperture (mm)	264	163	79
Quantity	5	5	4.5

MAGNET DESIGNS AND PARAMETERS

The aperture of magnet coil in this study was defined as $10\sigma_{max}$ plus 30 mm for the beam pipe (BP) and absorber (ABS) plus 3 mm for BP insulation and helium channel. In the IR magnets the coil aperture was increased by ~50 mm with respect to this definition and limited by two sizes, 320 mm in Q1 and 500 mm in Q2-Q4 and B1-B2, to reserve extra space for IR magnet protection against radiation [3]. The coil aperture of CS and adjacent MS magnets was increased to 270 mm, and in ARC magnets and adjacent MS magnets to 160 mm. This allows using thicker inner absorbers in arc magnets if necessary.
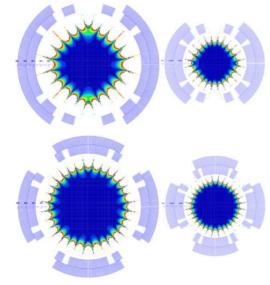

Figure 2: Coil cross-sections of HF SR dipoles (top) and quadrupoles (bottom) with 270 mm (left) and 160 mm (right) apertures.

The coil cross-sections were optimized with the ROXIE code [5] to achieve the required nominal operation field or gradient with margin and good field quality in the beam area of 8σ. As in our previous studies [3] the conceptual designs of the HF SR magnets are based on a 42-strand Rutherford cable, 21.6 mm wide and 1.85 mm thick, made of a 1 mm strand with Cu/nonCu ratio of 1.0. The cable is insulated with a 0.2 mm thick insulation.

All magnets are based on 2-layer, shell-type coils with remote iron yoke used mainly to reduce fringe fields. The optimized D and Q coil cross-sections for CS, MS and ARC sections are shown in Fig. 2.

The main magnet parameters at 4.5 K are reported in Table 5. Relatively low field level in CS, MS and ARC quadrupoles allows using the traditional NbTi technology. Therefore, the parameters of these magnets were calculated for both conductor options, NbTi and Nb$_3$Sn.

Table 5: Nominal Magnet Parameters at T_{op}=4.5 K

Parameter	Dipole		Quadrupole	
Coil ID (mm)	270	160	270	160
Max B_{op} (T)	10.0	10.0	-	-
B_{max} (T)	14.1	14.2	-	-
Max G_{op} (T/m)	-	-	33	36
G_{max} (T/m)	-	-	$54.1^*/96.6^\#$	$90.0^*/160.8^\#$
B_{max} coil (T)	15.8	15.6	$8.7^*/15.3^\#$	$8.3^*/14.7^\#$
Fraction of SSL	0.71	0.71	$0.61^*/0.34^\#$	$0.4^*/0.22^\#$
L (mH/m)	54.1	20.5	24.5	8.7
E_{op} (MJ/m)	4.33	1.84	0.59	0.12
F_{x_op} (MN/m)	9.25	5.98	0.89	0.25
F_{y_op} (MN/m)	-3.96	-2.66	-0.93	-0.28

* - NbTi; $^\#$ - Nb$_3$Sn

The Nb$_3$Sn dipole magnets operate at 71% and the quadrupoles at 22-34% of their short sample limit (SSL) at 4.5 K. Using the same cable with NbTi strand in both quadrupoles reduces G_{max} to 54 and 90 T/m. However, the magnets still have quite large operation margin, they operate at 61% and 40% of the SSL for 270 mm and 160 mm quads respectively. The final choice of the superconductor for SR quadrupoles will depend on the results of radiation studies for these magnets.

Geometrical field harmonics at the corresponding R_{ref} are reported in Table 6. With optimized coil cross-sections the relative field errors in the area occupied by muon beams is ~10^{-4} (dark blue area in Fig. 2).

Table 6: Geometrical Harmonics (10^{-4}).

	ID, mm	R_{ref}, mm	b_3	b_5	b_6	b_7	b_9	b_{10}
D	270	90	-0.2	-0.1	-	0.2	1.2	-
	160	53	0.0	-0.1	-	0.5	1.1	-
Q	270	90	-	-	0.2	-	-	0.0
	160	53	-	-	0.1	-	-	0.0

The dynamic aperture (DA) on the plane of transverse particle positions at the IP and projection of the IR quad aperture onto this plane using linear optics functions is shown in Fig. 3. The DA analysis with MADX PTC code shows that field errors (after correction) reduce DA by a factor of 2 to a size of the magnet good field region.
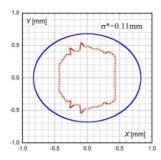
Figure 3: The dynamic aperture at IP and the projection of the IR quadrupole aperture (solid circle).

ENERGY DEPOSITION IN MAGNETS

Energy deposition and detector backgrounds induced by muon decays from both beams were simulated with MARS15 code [6] using our previous approach [7]. All the related details of geometry, materials and magnetic fields of the HF magnets in IR and SR were implemented in the 3D model along with a complete detector model, an optimized tungsten nozzle near IP and other components of the Machine-Detector Interface (Fig. 4).
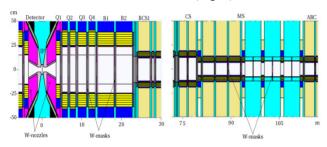

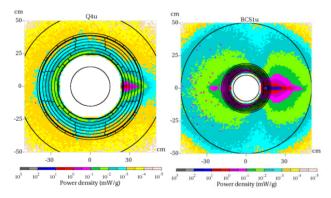Figure 4: MARS model of HF MDI, IR and SR.

Figure 5: Power density (mW/g) in the IP ends of the Q4 quadrupole (left) and $B_{CS}1$ dipole (right).

To protect IR and SR magnets, 15 cm long, 10σ ID tungsten masks were installed in the magnet interconnect regions. Inner absorbers include up to 10-mm thick stainless steel liners inside each magnet with additional tungsten segments in both horizontal and vertical planes in some magnets along the ring.

Power density distributions were calculated for each collider ring magnet. The protection system performs adequately in the IR quadrupoles where the peak power density P_p is at or below the quench limit of ~5 mW/g for Nb_3Sn coils [3] (Fig. 5, left). However, it is ~10 times

above the limit in B1 and B2 dipoles, and ~10^2 times above the limit for dipoles in CS, MS and ARC sections (Fig. 5, right). Additional tungsten inserts with the total radial thickness up to 5 cm, and a proper room for them in magnet apertures, are needed to reduce P_p below the limit.

Figure 6 shows the calculated dynamic heat load W_d in IR and SR magnets for both muon beams. The presented W_d values include both cold and potentially warm parts of magnet cross-section. The W_d in SR magnets is ~1 kW/m for the HF parameters of Table 1 except for the two dipoles at either end of the open section in MS and ARC, where it is ~2.5 kW/m. Note, that in spite of the low beam energy, the high number of decays in the HF keeps the level of W_d large as in the high energy machines [4], [7]. To reduce the W_d in the cold part of SR magnet system by ~100 times to the acceptable level of ~10 W/m, absorbers and masks have to be thermally insulated from the cold masses. It also requires extra space in magnet apertures.
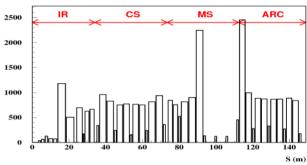

Figure 6: Dynamic heat load in IR and SR magnets.

SUMMARY

Preliminary design of HF based on the 125 GeV c.o.m. $\mu^+\mu^-$ collider including the IR and SR layout and the magnet system design concept was developed, and analysis of the beam dynamics and radiation issues was performed. It was found that protection of SR magnets from radiation and reduction of the dynamic heat load in the cold part of magnet cryostat present a serious problem and need further investigations and improvements including reiteration of the SR magnet system design.

REFERENCES

[1] Y. Alexahin et al., "A Muon Collider Higgs Factory for Snowmass 2013", arXiv:1308.2143v1 [hep-ph] 9 Aug 2013; Fermilab-Conf-13-245-T.

[2] D.V. Neuffer et al., "A Muon Collider as a Higgs Factory", Proc. of IPAC2013, Shanghai, China, May 2013, p. 1472.

[3] A.V. Zlobin et al., "Preliminary Design of a Higgs Factory $\mu^+\mu^-$ Storage Ring", ibid, p. 1487.

[4] Y.I. Alexahin et al., "Muon Collider Interaction Region Design", PRSTAB, 14, 061001 (2011).

[5] ROXIE, http://cern.ch/roxie/

[6] MARS15, http://www-ap.fnal.gov/MARS/

[7] N.V. Mokhov et al., "Muon Collider Interaction Region and Machine-Detector Interface Design", Proc. of PAC2011, NYC, March 2011, p. 82.